BIOCHEMISTRY

 Volume 43, Number 2 January 20, 2004

Articles

A Minimal Kinetic Model for a Viral DNA Packaging Machine†

Qin Yang‡ and Carlos Enrique Catalano*,‡,§

Department of Pharmaceutical Sciences and Molecular Biology Program, University of Colorado Health Sciences Center, Denver, Colorado 80262

Received August 26, 2003; Revised Manuscript Received October 28, 2003

ABSTRACT: Terminase enzymes are common to both eukaryotic and prokaryotic double-stranded DNA viruses. These enzymes possess ATPase and nuclease activities that work in concert to "package" a viral genome into an empty procapsid, and it is likely that terminase enzymes from disparate viruses utilize a common packaging mechanism. Bacteriophage λ terminase possesses a site-specific nuclease activity, a so-called helicase activity, a DNA translocase activity, and multiple ATPase catalytic sites that function to package viral DNA. Allosteric interactions between the multiple catalytic sites have been reported. This study probes these catalytic interactions using enzyme kinetic, photoaffinity labeling, and vanadate inhibition studies. The ensemble of data forms the basis for a minimal kinetic model for λ terminase. The model incorporates an ADP-driven conformational reorganization of the terminase subunits assembled on viral DNA, which is central to the activation of a catalytically competent packaging machine. The proposed model provides a unifying mechanism for allosteric interaction between the multiple catalytic sites of the holoenzyme and explains much of the kinetic data in the literature. Given that similar packaging mechanisms have been proposed for viruses as dissimilar as λ and the herpes viruses, the model may find general utility in our global understanding of the enzymology of virus assembly.

Virus development requires the coordinated synthesis of viral proteins and nucleic acid within the host cell and assembly of these macromolecules into an infectious virus particle (*1*−*3*). For double-stranded DNA (dsDNA)[1] viruses such as the eukaryotic herpes viruses and bacteriophage such as λ, T4, and SPP1, viral DNA is replicated as a linear concatemer of head-to-tail genomes (immature DNA) (*4*−*8*). Virus assembly requires the excision of a single (mature) genome from the concatemer and concomitant insertion of the DNA into a preformed capsid. Terminase enzymes are common to both eukaryotic and prokaryotic dsDNA viruses and are central to the packaging machine responsible for genome packaging and virus assembly. Common packaging mechanisms have been proposed for all of these enzymes. The terminase enzyme of bacteriophage λ has been intensively studied and provides an exceptional model system to define mechanistic aspects of genome packaging (*8*−*10*).

† This work was supported by National Institutes of Health Grant GM63943.

* Address correspondence to this author: (303) 315-6281 (fax); carlos.catalano@uchsc.edu (e-mail).

‡ Department of Pharmaceutical Sciences, School of Pharmacy.

§ Molecular Biology Program, School of Medicine.

[1] Abbreviations: AzATP, 8-azidoadenosine triphosphate; β-ME, 2-mercaptoethanol; *cos*, cohesive end site, the junction between individual genomes in immature concatemeric λ DNA; *cos*-cleavage reaction, the site-specific endonuclease activity of λ terminase; dsDNA, double-stranded DNA; *E. coli*, *Escherichia coli*; GMS, gel mobility shift; gpA, the large subunit of phage λ terminase; gpNu1, the small subunit of phage λ terminase; holoenzyme, the enzyme complex composed of terminase gpNu1 and gpA subunits; IHF, *Escherichia coli* integration host factor; kb, kilobase; kDa, kilodalton; SDS−PAGE, sodium dodecyl sulfate−polyacrylamide gel electrophoresis.

10.1021/bi035532h CCC: $27.50
Published on Web 12/19/2003

λ terminase is composed of gpA (73.3 kDa) and gpNu1 (20.4 kDa) subunits in a $gpA_1-gpNu1_2$ holoenzyme complex (*11*, *12*). Terminase introduces site-specific nicks into duplex DNA at a site known as *cos*, the packaging initiation site in the λ concatemer (*12*−*14*). The enzyme also possesses an ATP-dependent strand separation or so-called helicase activity that is required to generate a mature genome end suitable for packaging (*15*, *16*). Finally, the enzyme possesses a DNA translocase activity that is central to the packaging machine and that is responsible for insertion of viral DNA into the capsid (*17*−*19*). All of these catalytic activities reside in the larger gpA subunit of the holoenzyme. The gpA subunit further possesses an ATPase activity that regulates nuclease activity, that is required to drive strand separation, and that powers translocation of the packaging machinery during active DNA packaging (*8*, *20*, *21*). Site-specific assembly of the holoenzyme at *cos* is mediated by the gpNu1 subunit, a process that is also modulated by ATP (*22*).

Kinetic studies have demonstrated that both of the terminase subunits possess ATPase activity and have identified a high-affinity site in gpA ($K_m \approx 5$ μM) and a low-affinity site in gpNu1 [$K_m \approx 1.2$ mM (*21*, *23*)]. Moreover, studies on mutant terminase enzymes suggest that there are two ATPase centers in gpA: a C-terminal site including Lys497 that modulates nuclease activity and that is required for helicase activity (nuclease/helicase ATPase) (*24*) and an N-terminal site, including Tyr46 and Lys84, that is required for active DNA packaging (packaging ATPase) (*24*, *25*). Allosteric interactions between the ATPase catalytic sites and the nuclease and helicase catalytic sites of terminase holoenzyme have been described (*22*, *23*, *26*−*28*). While it is clear that these interactions are critical to the assembly of the packaging machinery onto viral DNA, to promoting stability of intermediate packaging complexes, and to modulating the procapsid-dependent transition to a mobile packaging machine (*8*, *29*), a mechanistic framework for these interactions is lacking. Central to our understanding of the packaging process is a description of the catalytic activities of the enzyme and the interactions between them. Here we report the results of enzyme kinetic, photoaffinity labeling, and vanadate inhibition studies that provide insight into the catalytic interactions required to assemble the packaging machinery onto viral DNA. A minimal kinetic model for terminase holoenzyme is proposed that incorporates allosteric interaction between the ATPase and nuclease sites in the assembly of the packaging machinery and preparation of the viral genome for packaging.

EXPERIMENTAL PROCEDURES

Materials and Methods. Radiolabeled nucleotides were purchased from Amersham-Pharmacia. Unlabeled nucleotides were purchased from Boehringer Mannheim Biochemicals. Mature λ DNA was purchased from Invitrogen. Vanadium oxide was purchased from Sigma Chemical Co. Stock solutions of VO_4^{3-} were prepared by the method of Goodno (*30*). Silica TLC plates were purchased from J. T. Baker. All other materials were of the highest quality commercially available.

Bacterial Strains, DNA Preparation, and Protein Purification. Plasmid pAFP1, kindly provided by M. Feiss (University of Iowa, Iowa City, IA), was purified from the *Escherichia coli* cell line JM107[pAFP1] using Qiagen DNA prep columns as described by the manufacturer. Purification of hexahistidine-tagged terminase holoenzyme and the isolated hexahistidine-tagged gpA subunit was performed as previously described (*31*). Phage λ procapsids were purified as described previously (*19*). *E. coli* integration host factor was purified from the overexpressing strain HN880 (generously provided by H. Nash, National Institutes of Health, Bethesda, MD) by the method of Nash et al. (*32*). All of our purified proteins were homogeneous as determined by SDS−PAGE.

Activity Assays. Unless otherwise indicated, the activity assays were performed as follows.

(A) The ATPase assay (10 μL) contained 50 mM Tris-HCl buffer, pH 9.0, 10 mM $MgCl_2$, 2 mM spermidine, 7 mM β-ME, 2 nM mature λ DNA, 50 μM [α-^{32}P]ATP (2 Ci/mmol), and 10 nM terminase holoenzyme. Vanadate was added as indicated in each individual experiment. The reaction was initiated with the addition of enzyme and was allowed to proceed for 20 min at 37 °C. The reaction was stopped with the addition of an equal volume of quench buffer (100 mM EDTA, 5 mM ATP, and 5 mM ADP), and the quenched reaction mixture was spotted on a silica gel TLC plate which was developed with buffer A (125 mL of 2-propanol, 60 mL of NH_4OH, and 15 mL of water). ADP formation at 20 min was quantified using a Molecular Dynamics phosphorimaging system and the ImageQuant software package as previously described (*23*, *26*).

(B) The cos-cleavage assay (10 μL) contained 20 mM Tris-HCl buffer, pH 8.0, 10 mM $MgCl_2$, 2 mM spermidine, 7 mM β-ME, 100 nM terminase, and 30 nM *Sca*I-linearized pAFP1 as the DNA substrate. ATP, IHF, and vanadate were added as indicated in each individual experiment. The reaction was initiated with the addition of enzyme and allowed to proceed at 37 °C for 60 min. The reaction was stopped with the addition of an equal volume of 100 mM EDTA, and the DNA was fractionated by 1% agarose gel. The ethidium bromide-stained products were analyzed by video densitometry as previously described (*12*, *33*).

(C) The DNA helicase assay (10 μL) contained 20 mM Tris-HCl buffer, pH 8.0, 11 mM $MgCl_2$, 1 mM ATP, 7 mM β-ME, 2 mM spermidine, 1 mM EDTA, and 5 nM *Acc*I-digested λ DNA (*16*). The reaction was initiated with the addition of terminase holoenzyme to a final concentration of 100 nM and allowed to proceed at 37 °C for 40 min. The reaction was then stopped with the addition of 3.4 μL of quench buffer (200 mM EDTA, 20% glycerol, 0.16% bromphenol blue, and 0.16% xylene cyanol), the DNA was fractionated on a 0.8% agarose gel, and the ethidium bromide-stained products were analyzed by video densitometry. Terminase-mediated strand separation of the *cos*-containing *Acc*I fragment yielded 5.6 and 2.2 kb products that were quantified using the Molecular Dynamics ImageQuant software package as previously described (*12*, *16*).

(D) The DNA packaging assay (20 μL) contained 50 mM Tris-HCl buffer, pH 8, 10 mM $MgCl_2$, 2 mM spermidine, 1 mM ATP, 30 nM IHF, 35 nM terminase, 1.5 nM mature λ DNA, and 15 nM procapsids. The reaction mixture was incubated at room temperature for 30 min, at which point DNase I was added to 10 μg/mL and the mixture was incubated for an additional 5 min. The reaction mixture was then extracted with phenol−chloroform, and the aqueous

phase was removed and analyzed by 0.8% agarose gel as previously described (*19*).

(E) The gel mobility shift (GMS) assay (10 μL) contained 20 mM Tris-HCl buffer, pH 8.0, 5 mM spermidine, 7 mM β-ME, and 30 pM radiolabeled 266mer as the *cos*-containing DNA substrate (*22*). Protein, ATP, and vanadate were included as indicated in each individual experiment. The mixture was incubated at room temperature for 20 min and then analyzed by 5% nondenaturing gel as described previously (*22*).

Affinity Labeling of Terminase with AzATP. Unless otherwise indicated, the binding buffer (20 μL) contained 50 mM Tris-HCl, pH 9.0, 10 mM $MgCl_2$, 1 μM λ terminase, and 2 mM [α-^{32}P]-8-azido-ATP (0.2 μCi/nmol, AzATP). The mixture was kept on ice for 3 min and then illuminated for 2 min with a hand-held UV lamp (254 nm at a distance of 4 cm). The reaction was stopped with the addition of an equal volume of quench buffer (100 mM EDTA and 10 mM DTT), and the proteins were fractionated by 15% SDS−PAGE. The protein bands were stained with Coomassie blue, and radioactive bands were visualized by phosphorimage analysis using a Molecular Dynamics Storm system. Radioactivity incorporated into each protein was quantified using the Molecular Dynamics ImageQuant software package.

RESULTS

DNA Stimulates Steady-State ATPase Activity. Both subunits in terminase holoenzyme hydrolyze ATP, with K_m's of 5 μM and 1.2 mM for gpA and gpNu1, respectively, in the absence of DNA (*21*, *23*). Thus, at a concentration of 50 μM, ATP hydrolysis is essentially limited to the gpA subunit of the holoenzyme. We have previously demonstrated that DNA stimulates the ATPase activity of gpA in the holoenzyme complex (*26*, *31*), and this result is reproduced in Figure 1A. Under the conditions used in this study, DNA stimulates the steady-state rate of ATP hydrolysis ≈7-fold. Conversely, the isolated gpA subunit possesses a weak ATPase activity that is unaffected by DNA (*20*, *26*, *31*). These data demonstrate that quaternary interactions between gpA and gpNu1 in the holoenzyme complex are required for the full expression of gpA ATPase activity and for the observed stimulation by DNA.

Increasing the ATP concentration to 1 mM promotes binding and hydrolysis at gpNu1, and both subunits in the holoenzyme are catalytically active. Under these conditions, DNA stimulates the steady-state rate of ATP hydrolysis by 17-fold (Figure 1B), which is significantly greater than the 7-fold increase observed at the gpA subunit. This result is consistent with the observation that DNA also strongly stimulates ATP hydrolysis at the gpNu1 subunit of the holoenzyme (*21*, *23*, *26*). Importantly, the isolated gpNu1 subunit possesses only modest ATPase activity and DNA has no effect (*20*, *33*), again demonstrating that interactions between the holoenzyme subunits are required for the full expression of catalytic activity in both subunits.

Vanadate Inhibits Steady-State ATP Hydrolysis. Vanadate is a phosphate analogue that has been shown to inhibit the ATPase activity of a number of enzymes, and this compound has been successfully used as a mechanistic probe of ATPase catalytic mechanisms (*30*, *34*). Vanadate inhibition of the ATPase and DNA packaging activities of λ terminase has been demonstrated (*20*); however, a detailed investigation of the effects of vanadate on the multiple, ATP-modulated activities of terminase has not been performed.

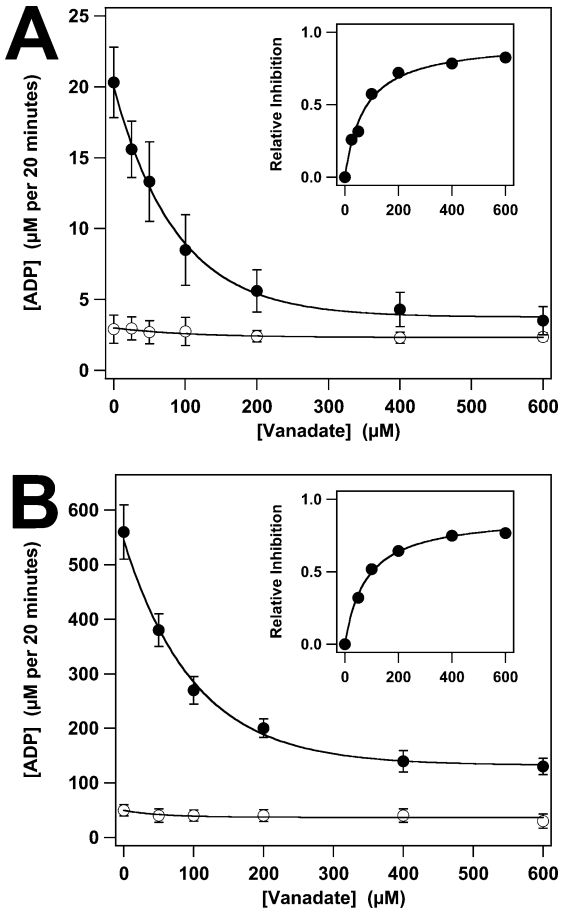

FIGURE 1: Steady-state ATPase activity. The ATPase assay was conducted as described in Experimental Procedures, and the amount ADP formed in 20 min was determined. Each data point represents the average of three separate experiments, with the standard deviation indicated with error bars. Panel A: Terminase holoenzyme and ATP were included at a concentration of 10 nM and 50 μM, respectively. Reactions were conducted in the absence (○) or presence (●) of DNA, and vanadate was included as indicated. The inset shows a replot of the plus DNA data, indicating the relative inhibition by vanadate. The data were fit to a hyperbolic curve function, yielding $K_{I,app} = 74 \pm 11$ μM for vanadate inhibition of DNA-stimulated ATPase activity. Panel B: Terminase and ATP were included at 200 nM and 1 mM, respectively, in the absence (○) and presence (●) of DNA. Vanadate was included as indicated. The inset shows a replot of the plus DNA data, indicating the relative inhibition by vanadate. Analysis of the data as described above yields $K_{I,app} = 80 \pm 6$ μM.

We first examined the effect of vanadate on the steady-state rate of ATP hydrolysis by gpA in the holoenzyme complex using 50 μM ATP. Under these conditions, vanadate does not affect basal ATP hydrolysis but completely abolishes the capacity of DNA to stimulate the reaction (Figure 1A). This trend was observed at vanadate concentrations as high as 10 mM (not shown). Interestingly, vanadate only modestly affects ATP hydrolysis by the isolated gpA subunit, in both the absence and presence of DNA (data not shown). This suggests that DNA stimulation and vanadate inhibition are linked events that likely require quaternary interaction between the subunits in terminase holoenzyme.

As described above, increasing the ATP concentration to 1 mM promotes binding and hydrolysis at the gpNu1

Table 1: Effect of Vanadate on Terminase Catalytic Activities[a]

reaction	[nucleotide]	vanadate $K_{I,app}$
basal ATPase	50 μM ATP	<10%[b]
DNA-stimulated ATPase	50 μM ATP	74 ± 11 μM[b]
basal ATPase	1 mM ATP	<10%[b]
DNA-stimulated ATPase	1 mM ATP	80 ± 6 μM[b]
basal DNA binding	none	<5%[c]
ATP-stimulated DNA binding	1 mM ATP	<5%[c]
basal nuclease	none	<5%[d]
ATP-stimulated nuclease	1 mM ATP	105 ± 13 μM[d]
ADP-stimulated nuclease	1 mM ADP	107 ± 10 μM
helicase activity	50 μM ATP	64 ± 9 μM[e]
DNA packaging activity	1 mM ATP	444 ± 8 μM[f]

[a] Assays for catalytic activities were performed as described in Experimental Procedures with nucleotide added as indicated in the table. [b] Data taken from Figure 1. Inhibition of basal ATPase activity was not detectable within the experimental error of the assay (≈10%). [c] Data taken from Figure 3. Inhibition of DNA binding affinity was not detectable within the experimental error of the assay (≈5%). [d] Data taken from Figure 5A. Inhibition of basal nuclease activity was not detectable within the experimental error of the assay (≈5%). [e] Data taken from Figure 6A. [f] Data taken from Figure 7.

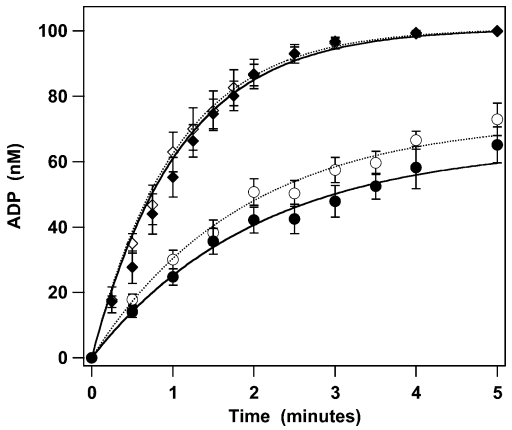

FIGURE 2: Single-turnover ATP hydrolysis by gpA in the holoenzyme complex. The ATPase activity assay was performed as described in Experimental Procedures, except that terminase holoenzyme and ATP were included at 200 and 100 nM, respectively. Each data point represents the average of three separate experiments, with the standard deviation indicated with error bars. The reaction was performed in the absence (○) or presence (◇) of DNA. Addition of 800 μM sodium vanadate to the reaction mixture had little effect on the observed rate of the reaction in either the absence (●) or presence (◆) of DNA. The solid curves represent the best fit of the data to a single-exponential curve function. The results are presented in Table 2.

catalytic site. Identical results are observed under these conditions; vanadate does not affect basal ATPase activity but completely abolishes the capacity of DNA to stimulate the reaction. We note that the $K_{I,app}$ is essentially identical under both experimental conditions (50 μM vs 1 mM ATP; Table 1).

Single-Turnover ATP Hydrolysis by gpA in Terminase Holoenzyme. We next examined the hydrolysis of ATP by the terminase gpA subunit in a single-turnover experiment; ATP was added at a concentration of 100 nM, and the reaction was initiated with the addition of holoenzyme to a final concentration of 200 nM. Under these conditions, a single catalytic turnover is observed. Moreover, the reaction is limited to the gpA subunit of the holoenzyme due to the low concentration of ATP used (vide supra). Figure 2 shows that gpA in the holoenzyme complex hydrolyzes ATP with

Table 2: Effect of DNA and Vanadate on the Observed Single-Turnover Rate of ATP Hydrolysis by gpA in Terminase Holoenzyme[a]

[DNA] (nM)	[vanadate] (μM)	obsd rate (min^{-1})
0	0	0.54 ± 0.07
2	0	0.97 ± 0.05
0	800	0.49 ± 0.08
2	800	0.93 ± 0.04

[a] Data taken from Figure 2.

an observed rate of 0.54 ± 0.07 min^{-1} and that DNA has only a modest effect on the reaction (Table 2). This <2-fold stimulation is significantly less than the 7-fold stimulation observed under steady-state conditions (see Figure 1A). Furthermore, in stark contrast to the effects observed under steady-state conditions, vanadate has no significant effect on the observed rate of ATP hydrolysis in a single catalytic turnover in either the absence or presence of DNA (Figure 2, Table 2).

Effect of ATP on Terminase−DNA Binding Interactions. We previously demonstrated that 1 mM ATP increases the affinity of gpNu1 for *cos*-containing DNA (*22*), and this result is reproduced in Figure 3A.[2] The K_m for ATP hydrolysis by gpNu1 is 500 μM [in the presence of DNA (*21*, *23*)], which predicts that high micromolar concentrations of nucleotide are required to bind to the protein and thus affect DNA binding. Consistently, 50 μM ATP does not affect gpNu1 binding to *cos*-DNA (not shown).

ATP (1 mM) does not affect binding of the gpA subunit to DNA but significantly increases binding of the holoenzyme to *cos*-DNA (panels B and C of Figure 3, respectively). This increase in terminase binding affinity is presumably mediated by the gpNu1 subunit. Consistently, 50 μM ATP does not affect holoenzyme binding to *cos*-DNA (not shown). In summary, the data demonstrate that ATP binding to gpNu1 increases binding of the holoenzyme to DNA.

Effect of Vanadate on Terminase−DNA Binding Interactions. The data presented in Figure 1 demonstrate that vanadate abrogates the capacity of DNA to stimulate steady-state ATP hydrolysis by terminase holoenzyme. A feasible mechanism for this observation is that vanadate inhibits DNA binding. Thus, the effect of vanadate on terminase−DNA binding interactions was investigated.

The data show that vanadate does not affect binding of the terminase proteins, alone or in combination, to *cos*-DNA (Figure 3, Table 3). It is important to note that ATP continues to stimulate terminase binding to DNA in the presence of vanadate (Figure 3). This result strongly suggests that ATP binding to gpNu1 is unaffected by vanadate in this concentration range. The effect of vanadate on ATP binding to terminase is examined in more detail below.

Photoaffinity Labeling of Terminase Holoenzyme with 8-Azido-ATP (AzATP). While it has been demonstrated that DNA stimulates ATP hydrolysis at both enzyme subunits (*23*, *31*), the effect of DNA on ATP binding interactions has not been examined. AzATP has been used as a photoaffinity probe for a variety of ATP binding proteins

[2] Binding of gpNu1 to nonspecific DNA substrates does not occur under the conditions used in this study, and ATP has no observable effect on this interaction (M. Ortega and C. E. Catalano, unpublished results).

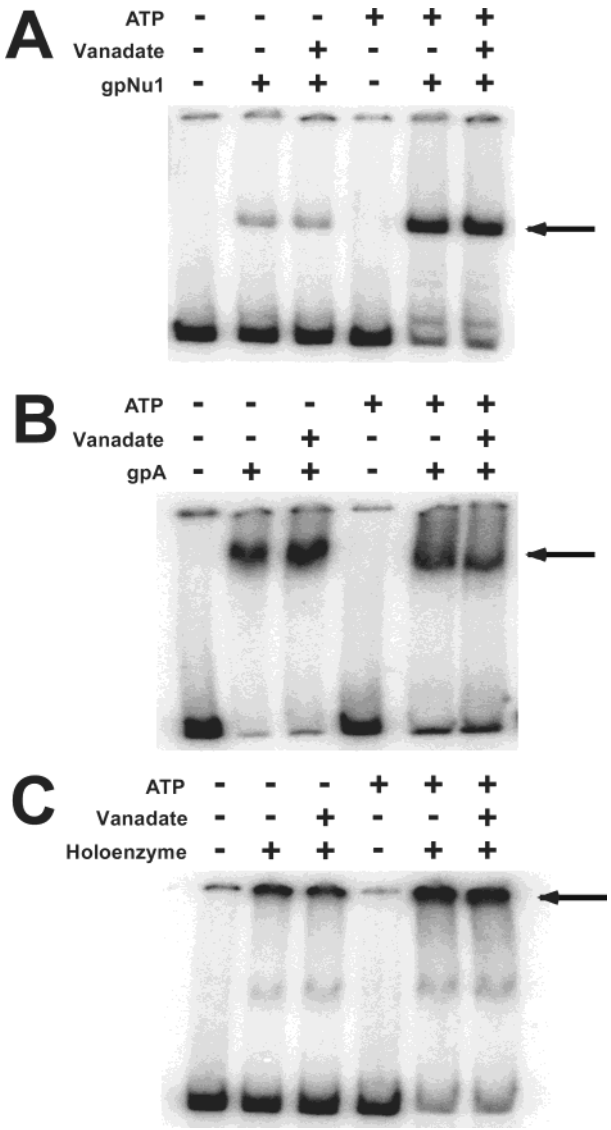

FIGURE 3: Vanadate does not affect DNA binding activity. Panel A: The GMS assay was performed as described in Experimental Procedures using 25 nM purified gpNu1. Panel B: The GMS assay was performed as described in Experimental Procedures using 500 nM purified gpA. Panel C: The GMS assay was performed as described in Experimental Procedures using 50 nM terminase holoenzyme. ATP and vanadate were included at 1 mM and 800 μM, respectively, as indicated. The figure shows representative results obtained from three separate experiments. The data from the three experiments were quantified as described previously (*22*), and the results are presented in Table 3.

Table 3: Sodium Vanadate Does Not Affect Terminase DNA Binding Affinity[a]

protein	[vanadate] (μM)	% DNA shifted
gpNu1	0	75 ± 4
gpNu1	800	73 ± 4
gpA	0	83 ± 5
gpA	800	80 ± 6
holoenzyme	0	81 ± 2
holoenzyme	800	78 ± 3

[a] The data presented in Figure 3 (plus ATP) were analyzed as described in Experimental Procedures. The results represent the average of three independent experiments.

(*35*), and this probe has been previously utilized to covalently modify ATP binding sites in both subunits of terminase holoenzyme (*21*, *25*, *36*). Consistent with these published

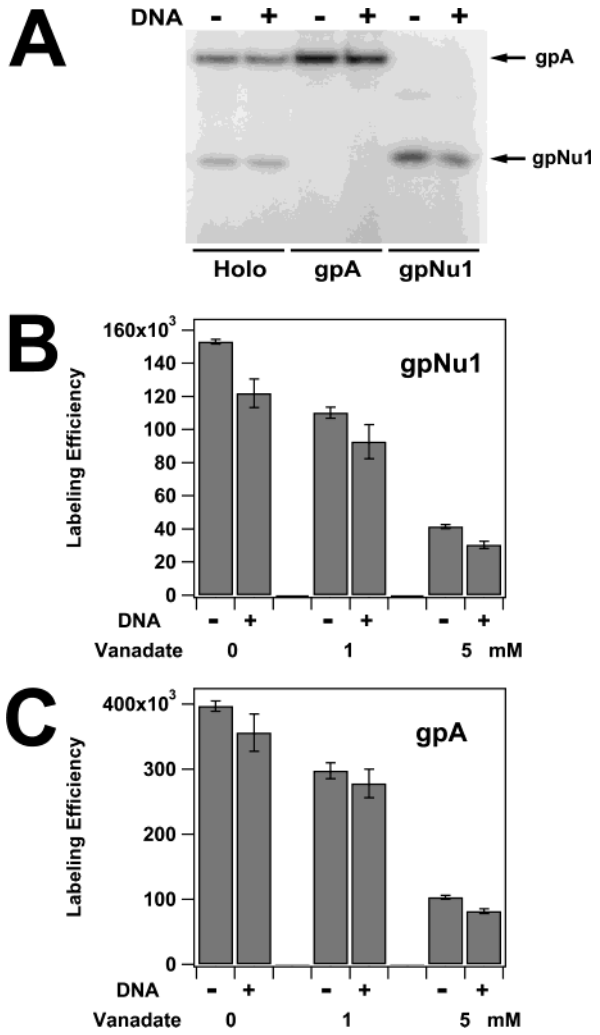

FIGURE 4: Vanadate attenuates AzATP photoaffinity labeling of the terminase subunits. Terminase holoenzyme was covalently modified with AzATP as described in Experimental Procedures. Mature λ DNA (1.5 nM) and vanadate were added to the photolysis mixture as indicated. Panel A: Representative phosphorimage of radiolabeled proteins fractionated by PAGE. The position of the terminase subunits in the gel is indicated with arrows. Panel B: Photolabeling of the gpNu1 subunit in terminase holoenzyme was quantified by phosphorimage analysis as described. The photolysis mixtures contained DNA and/or vanadate as indicated. The results represent the average of three separate experiments, with the standard deviation indicated with error bars. Panel C: Photolabeling of the gpA subunit in terminase holoenzyme was quantified by phosphorimage analysis as described. The photolysis mixtures contained DNA and/or vanadate as indicated. The results represent the average of three separate experiments, with the standard deviation indicated with error bars.

data, Figure 4A shows that AzATP at a concentration of 2 mM efficiently labels both of the terminase subunits, alone and in the holoenzyme complex. Analysis of the data reveals that the gpA subunit is labeled with a 2.5−3-fold higher efficiency relative to gpNu1 under these conditions. Interestingly, while DNA stimulates ATP hydrolysis 17-fold under these conditions (see Figure 1), polynucleotide does not affect AzATP labeling of either subunit and, in fact, may slightly inhibit nucleotide binding (Figure 4B,C). While 800 μM vanadate does not affect ATP binding to the enzyme (vide supra), elevated concentrations inhibit AzATP labeling of both terminase subunits in a concentration-dependent manner, in both the absence and presence of DNA (Figure 4).

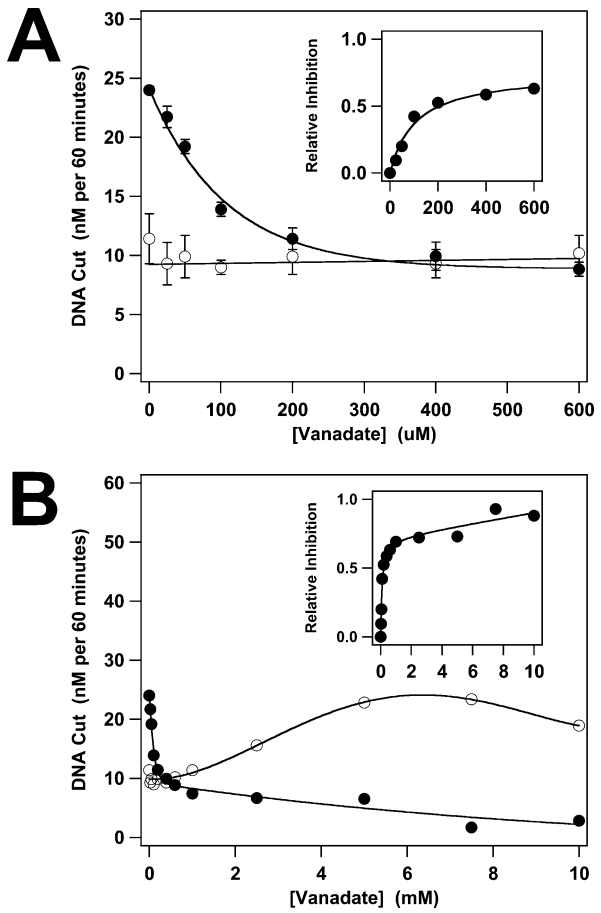

FIGURE 5: Vanadate inhibits ATP-stimulated terminase nuclease activity. The *cos*-cleavage assay was conducted as described in Experimental Procedures, and the amount DNA cut in 60 min was determined. Panel A: The *cos*-cleavage assay was performed in the absence (○) or presence (●) of 1 mM ATP and with vanadate added as indicated. The inset shows a replot of the plus ATP data, indicating the relative inhibition by vanadate. The data were fit to a hyperbolic curve function, yielding $K_{I,app} = 105 \pm 13$ μM for vanadate inhibition of ATP-stimulated nuclease activity. Panel B: The *cos*-cleavage assay was performed as described in the absence (○) or presence (●) of 1 mM ATP and with vanadate added as indicated. The inset shows a replot of the plus ATP data, indicating the relative inhibition by vanadate.

Essentially identical results were observed using 50 μM AzATP, except that labeling of the gpNu1 subunit decreased 30−40-fold (data not shown).

Adenosine Nucleotides Stimulate Nuclease Activity. Terminase holoenzyme possesses a site-specific endonuclease activity that is stimulated by ATP (*26*, *27*, *37*). Under the conditions used in this study, both ATP and ADP stimulate the nuclease reaction 2−3-fold (Figure 5A and data not shown). Importantly, 50 μM ATP is sufficient to fully stimulate nuclease activity (Table 4). Thus, nucleotide binding to the gpA subunit is responsible for stimulation of the nuclease activity of the enzyme. This is distinct from nucleotide binding to gpNu1, which is responsible for increasing the affinity of the enzyme for DNA (see above).

Sodium Vanadate Inhibits ATP-Stimulated Nuclease Activity. We next investigated the effect of vanadate on the nuclease activity of the enzyme. The data show some interesting features, as follows.

(i) At low concentrations (≤600 μM), vanadate inhibits ATP-stimulated nuclease activity but has little effect on basal nuclease activity (Figure 5A). Identical results were obtained with ADP (Table 1). Thus, vanadate inhibition of ATP-stimulated nuclease activity exhibits a pattern essentially identical to that observed for the DNA-stimulated ATPase activity of the enzyme. That is, vanadate inhibits stimulated activity but does not affect basal catalytic activity. Indeed, the $K_{I,app}$ for vanadate inhibition is similar in both cases (Table 1).

Table 4: Sodium Vanadate Inhibits ATP-Stimulated Nuclease Activity[a]

[ATP]	[vanadate] (μM)	relative activity[b]
none	0	1
50 μM	0	2.3
1 mM	0	2.5
none	800	1.1
50 μM	800	1.2
1 mM	800	1.4

[a] The *cos*-cleavage reaction was performed as described in Experimental Procedures with ATP and vanadate added as indicated in the table. [b] A relative activity of 1 corresponds to 30% of the input DNA cleaved at 60 min.

(ii) Increasing the concentration of vanadate above 600 μM has paradoxical effects on terminase nuclease activity, depending on whether nucleotide is included in the reaction mixture. In the presence of ATP, vanadate continues to inhibit the reaction, though the concentration dependence is less striking than at lower concentrations (Figure 5B). Identical results were obtained with ADP (not shown). The clear break in the concentration dependence at ≈600 μM strongly suggests that vanadate inhibits ATP-stimulated nuclease activity via two discrete mechanisms.

(iii) Inhibition of basal nuclease activity in the absence of nucleotide is remarkable. While low vanadate concentrations (≤600 μM) have little effect, elevated concentrations *stimulate* the reaction (Figure 5B). The clear break in the concentration curve at ≈600 μM is consistent with two discrete effects of vanadate on nuclease activity. Finally, we note that sodium phosphate had no effect on the nuclease activity of the enzyme in either the absence or presence of ATP (data not shown).

Interaction between ATP and IHF in Stimulation of Terminase Nuclease Activity. We previously reported that ATP did not affect the *cos*-cleavage reaction in vitro (*12*). This result is in stark contrast to published literature (*27*, *37*) and to the data presented here (Figure 5). A critical difference between our early experiments and those reported here is the absence or presence of *E. coli* integration host factor (IHF). IHF stimulates virus yield in vivo (*38*−*40*), and we have previously demonstrated that IHF stimulates the nuclease activity of terminase holoenzyme 2−3-fold in vitro (*12*). This experiment was reproduced here, and the results are presented in Table 5. The table further demonstrates that ATP has little effect on nuclease activity in the presence of IHF. Thus, the discrepancy between our initial report and those reported here and in the literature is attributable to differences in reaction conditions, specifically the absence or presence of IHF. Table 5 further shows that vanadate has no significant effect on the capacity of IHF to stimulate the nuclease activity of λ terminase.

Sodium Vanadate Inhibits Terminase Helicase Activity. ATP hydrolysis at the gpA subunit is required to separate

Table 5: Sodium Vanadate Does Not Affect IHF-Stimulated Nuclease Activity[a]

[ATP] (mM)	[IHF] (nM)	[vanadate] (μM)	relative activity[b]
0	0	0	1
0	100	0	2.9
1	100	0	3.2
0	100	800	2.9
1	100	800	2.1

[a] The *cos*-cleavage assay was conducted as described in Experimental Procedures with ATP, IHF, and vanadate added as indicated in the table. [b] A relative activity of 1 corresponds to 25% of the input DNA cleaved at 60 min.

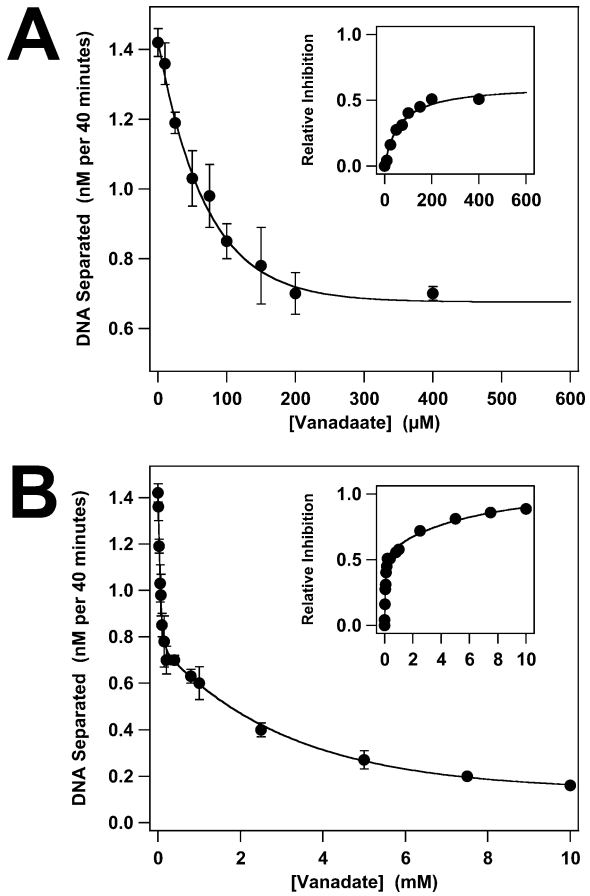

FIGURE 6: Vanadate inhibits the helicase activity of λ terminase. Panel A: The helicase assay was performed as described in Experimental Procedures with vanadate added as indicated. Each data point represents the average of three separate experiments, with the standard deviation indicated with error bars. The inset shows a replot of the data, indicating the relative inhibition by vanadate. The data were fit to a hyperbolic curve function, yielding $K_{I,app} = 64 \pm 9$ μM for vanadate inhibition of helicase activity. Panel B: The helicase assay was performed as described with vanadate added as indicated. The inset shows a replot of the plus ATP data, indicating the relative inhibition by vanadate.

the nicked, annealed strands created by the nuclease activity of terminase holoenzyme, and we next examined the effect of vanadate on this so-called "helicase" activity. Figure 6A demonstrates that low concentrations of vanadate (≤600 μM) strongly inhibit the helicase activity of terminase. The $K_{I,app}$ for vanadate observed in this concentration range is quite similar to that observed for inhibition of ATPase and nuclease catalytic activities (see Table 1). This suggests that low concentrations of vanadate abrogate all three catalytic activities via a common mechanism. Elevated vanadate

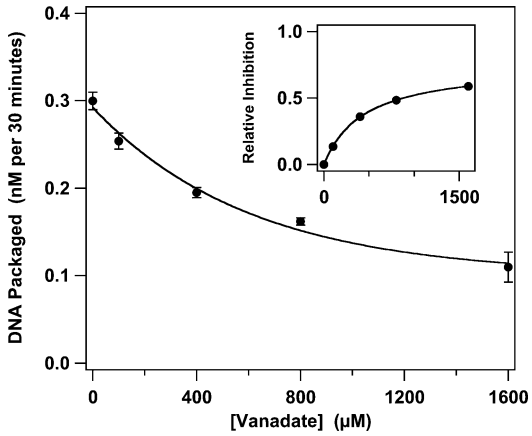

FIGURE 7: Vanadate inhibits the DNA packaging activity of λ terminase. The in vitro packaging assay was performed as described in Experimental Procedures with vanadate added as indicated. Each data point represents the average of three separate experiments, with the standard deviation indicated with error bars. The inset shows a replot of the data, indicating the relative inhibition by vanadate. The data were fit to a hyperbolic curve function, yielding $K_{I,app} = 444 \pm 8$ μM for vanadate inhibition of DNA packaging activity.

concentrations continue to inhibit helicase activity, though the concentration dependence is not as striking (Figure 6B). This result is virtually identical to that observed for the ATP-stimulated nuclease activity of the enzyme (compare Figure 5B inset and Figure 6B inset) and is consistent with the suggestion that (i) the nuclease and helicase activities of the enzyme are coupled and that (ii) vanadate affects the enzyme via two discrete mechanisms.

Sodium Vanadate Inhibits in Vitro DNA Packaging. The genome packaging activity of λ terminase is likely driven by ATP hydrolysis at a gpA catalytic site (*8*, *24*). It is thus reasonable that vanadate-mediated inhibition of ATP hydrolysis would affect genome packaging. Indeed, vanadate inhibition of λ terminase packaging activity has been previously demonstrated (*17*). The data presented in Figure 7 show that this inhibition is concentration-dependent. Importantly, the $K_{I,app}$ for vanadate inhibition of packaging activity is significantly greater than that observed for inhibition of the DNA-stimulated ATPase, ATP-stimulated nuclease, and DNA helicase activities of the holoenzyme (Table 1).

DISCUSSION

Double-stranded DNA viruses such as the herpes viruses and many bacteriophage replicate their DNA as linear concatemers several genomes in length (*4*−*8*). Terminase enzymes are common to these viruses and are required to package monomeric genomes from the concatemeric precursors (*2*, *5*, *8*, *41*). The terminase enzymes from these viruses, where characterized, are composed of two subunits and possess ATPase and nuclease activities that work in concert to package viral DNA (*5*, *7*, *8*). In bacteriophage λ, the smaller gpNu1 subunit possesses ATPase activity and is required for site-specific assembly of the packaging machinery at *cos* (*21*−*23*, *26*, *31*). The nuclease, helicase, and DNA packaging activities of the holoenzyme reside in the larger gpA subunit, which also possesses ATPase activity (*16*, *21*, *26*, *31*, *33*). While it is clear that the catalytic sites work in concert to effect DNA packaging, a mechanistic description

of these interactions and of their role in the assembly of the packaging machinery remains obscure. Moreover, a comprehensive kinetic model for the coordinated catalytic activities of the enzyme is lacking. We therefore performed a variety of studies directed toward defining interactions between the multiple catalytic sites of the holoenzyme.

Allosteric Interactions in Terminase Holoenzyme. A minimal kinetic model for terminase holoenzyme must accommodate a nuclease, a helicase, and DNA packaging activity in the gpA subunit and a site-specific DNA binding activity in gpNu1. The model must also address three ATPase catalytic sites: one associated with DNA packaging activity located in the N-terminus of gpA (the packaging ATPase), a second associated with the nuclease and helicase activities and located in the C-terminus of gpA (N/H ATPase), and a third ATPase site located in the gpNu1 subunit.[3] Furthermore, the model must incorporate the following observations. (i) ATP binding to gpNu1 increases the affinity of the holoenzyme for *cos*-DNA (Figure 3). (ii) ATP stimulates the nuclease activity of the holoenzyme but through distinct interactions with the gpA subunit (Table 4). (iii) DNA strongly stimulates steady-state ATP hydrolysis at both subunits of the holoenzyme (Figure 1) but does not promote nucleotide binding at either (Figure 4). (iv) While DNA stimulates the steady-state rate of ATP hydrolysis at gpA, it only modestly affects single-turnover ATP hydrolysis by the subunit (Figure 2). Thus, DNA stimulates ATP hydrolysis by increasing the rate of product release and/or by increasing the rate of a post-chemistry rate limiting conformational change step. (v) At low concentrations ($\leq$600 μM), vanadate inhibits both DNA-stimulated ATPase and ATP-stimulated nuclease activities but not basal catalytic activities (Figures 1 and 5). Moreover, vanadate similarly inhibits helicase activity at these concentrations (Figure 6), and the $K_{I,app}$ is quite similar in all three cases (Table 1). This suggests that the three processes are mechanistically linked. (vi) Vanadate does not affect the single-turnover ATPase activity of the gpA subunit (Figure 2), which indicates that it exerts its effect after ATP hydrolysis. Finally, we note that full expression of the nuclease, helicase, and ATPase catalytic activities of gpA requires the presence of gpNu1 and that DNA stimulation of ATP hydrolysis is only observed in the holoenzyme complex. Thus, quaternary interactions between the subunits are required for communication between all of the catalytic sites.

A Minimal Kinetic Model for Terminase Holoenzyme. We propose the following kinetic model for terminase holoenzyme that is harmonious with the data presented here and that in the literature. Initially, terminase is in a low (basal) activity state where the nuclease activity of the holoenzyme is slow and inaccurate and where both enzyme subunits slowly hydrolyze ATP (Scheme 1, rectangular subunits). Steady-state ATP hydrolysis by gpA occurs at the packaging ATPase catalytic site. This is based on the observation that (i) mutation of residues that inactivate the basal ATPase activity of gpA also inactivate the packaging activity of the enzyme and that (ii) mutation of residues that inactivate nuclease and helicase activities only modestly affect basal ATPase activity (*21*, *24*, *28*).

The data indicate that ATP and DNA act in concert to yield an activated holoenzyme where both ATP hydrolysis and duplex nicking reactions are stimulated. We propose the following sequence of events to explain the data (Scheme 1). (i) ATP binding to gpNu1 increases the affinity of *cos*-DNA for the subunit. This initiates holoenzyme assembly at *cos*. (ii) ATP also binds to the nuclease/helicase (N/H) ATPase site in gpA. Hydrolysis at this site yields the ternary gpA−ADP−DNA complex. (iii) ADP drives a conformational reorganization in the quaternary structure of the holoenzyme thus assembled, yielding an activated nuclease complex of high fidelity (oval subunits, Scheme 1). Fast and accurate nicking of the duplex ensues, and the helicase activity of gpA separates the nicked, annealed strands yielding complex I. ATP hydrolysis at both subunits is also stimulated in this activated complex, and this is discussed further below.

ADP Modulates the Conformational Reorganization. Evidence for a DNA and ADP (vs ATP) triggered conformational change to an activated complex is provided by a number of observations. First, DNA strongly stimulates the steady-state ATPase activity of gpA but only modestly affects ATP hydrolysis in a single catalytic turnover. This indicates that DNA does not affect ATP binding or hydrolysis steps. Rather, DNA exerts its predominant effect *after* the chemical step (ATP hydrolysis) and implicates an ADP-bound intermediate. Second is the observation that vanadate does not inhibit the single-turnover ATP hydrolysis reaction but strongly inhibits DNA-stimulated steady-state hydrolysis. This indicates that vanadate also exerts its effect after the chemical step. Third, ATP and ADP similarly stimulate the nuclease activity of terminase holoenzyme, and essentially identical $K_{I,app}$'s for vanadate inhibition are obtained with both nucleotides. This suggests that ADP (formed from the hydrolysis of ATP or added directly) is the pertinent species. Finally, we note that this model is fully consistent with known mechanisms of inhibition, where vanadate binds to the enzyme−ADP complex after ATP hydrolysis and phosphate release forming a ternary enzyme−ADP−VO_4^{3-} complex (*30*, *34*). Importantly, the micromolar $K_{I,app}$ for vanadate inhibition observed in our study is consistent with this type of inhibition mechanism (*30*, *34*, *42*). Unlike many of these systems, however, vanadate does not form a long-lived inhibition complex with terminase (data not shown). The absence of a long-lived terminase−ADP−VO_4^{3-} complex indicates that dissociation of ADP−VO_4^{3-} and/or DNA from the enzyme is relatively fast and presumably reversible. Thus, basal ATPase activity is unaffected by vanadate.

Mechanism for Vanadate Inhibition of Terminase Catalytic Activities. Vanadate inhibits the coordinated DNA- and ATP-stimulated activities of terminase holoenzyme without affecting basal catalytic activity, and the data are consistent with inhibition via an enzyme−ADP−VO_4^{3-} ternary complex. To accommodate these data, we suggest that vanadate

[3] Genetic, biochemical, and kinetic studies indicate that terminase holoenzyme possesses two ATPase catalytic sites, one in gpA and a second in gpNu1 (*21*, *23*, *26*, *31*). Recent studies further suggest (but do not prove) that two discrete ATP binding sites reside in the gpA subunit (*24*). Fluorescence-monitored nucleotide binding studies provide support for a second ATP binding site in gpA (Gaussier and Catalano, work in progress). We therefore presume that terminase holoenzyme possesses two discrete ATP binding sites in gpA: an N-terminal site associated with packaging activity and a C-terminal site directly involved with the nuclease and helicase activities of the holoenzyme, as described in the model. We note, however, that the third site has not been rigorously demonstrated.

Scheme 1: Minimal Kinetic Model for Terminase Holoenzyme

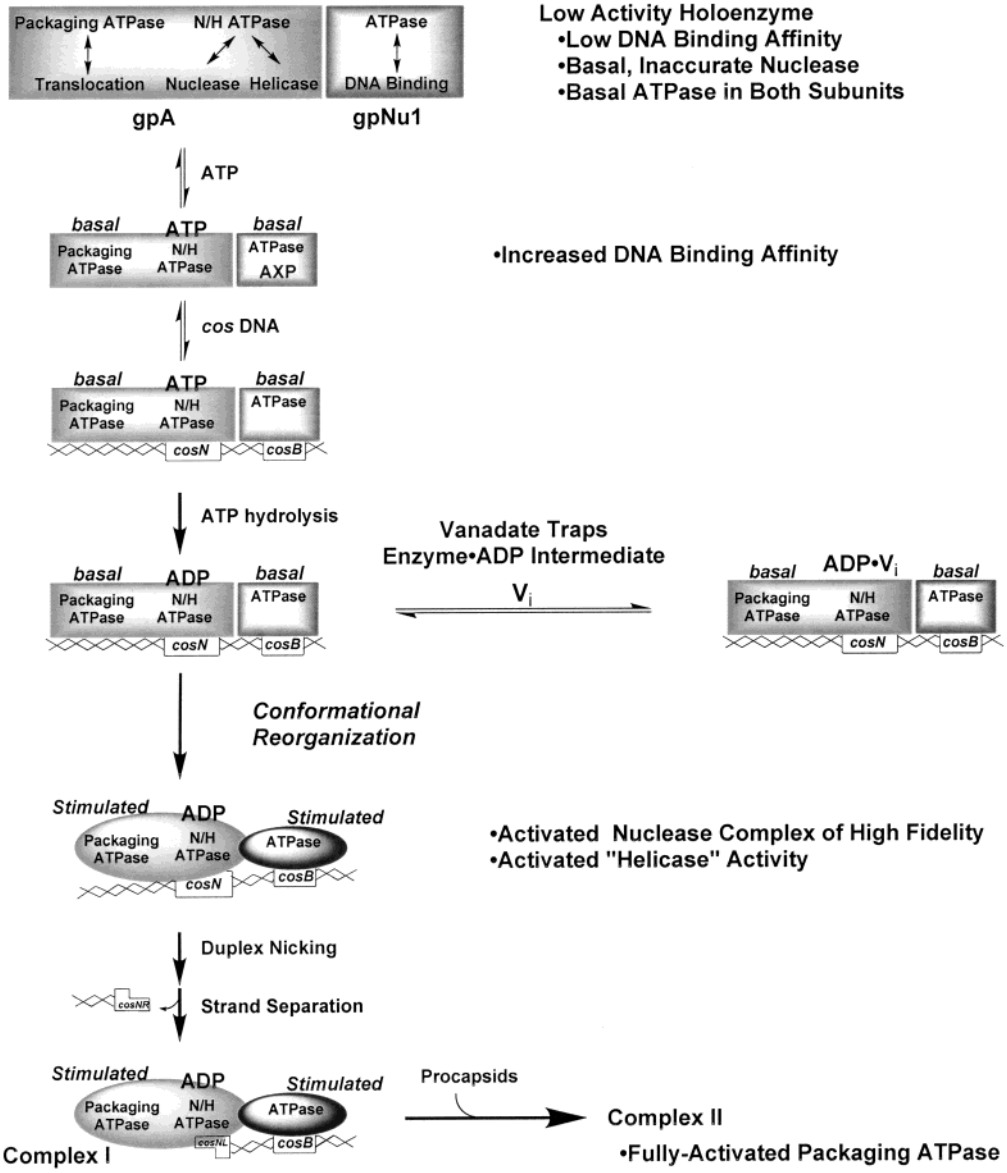

[a] Terminase holoenzyme is represented at the top as rectangles (designated gpA and gpNu1). The subunit stoichiometry in terminase holoenzyme remains speculative, and none is intended. The packaging, nuclease, and helicase catalytic sites in gpA are indicated, as is the site-specific DNA binding site in gpNu1. The three ATPase catalytic sites are also indicated (N/H ATPase represents the nuclease/helicase ATPase catalytic site). Initially, terminase is in a low-activity state. Basal ATP hydrolysis at the packaging ATPase site in gpA and the ATPase site in gpNu1 is indicated above each subunit. Basal nuclease activity is slow and inaccurate. ATP binding to gpNu1 increases the affinity of the holoenzyme for *cos*-DNA. (ATP bound at the gpNu1 ATPase site is hydrolyzed to ADP, and nucleotide bound to gpNu1 is thus represented as AXP, shown explicitly only in the first intermediate for simplicity). Terminase assembles at the *cos* site of a viral concatemer. *CosN* and *cosB* are subsites where duplex nicking and gpNu1 assembly take place, respectively. ATP hydrolysis by the N/H ATPase site yields ADP, which triggers a conformational reorganization of the terminase subunits assembled onto DNA. This yields an activated nuclease complex of high fidelity and a high-affinity single-stranded binding complex that is responsible for helicase activity. Procapsid capture by complex I fully activates the packaging ATPase site in gpA and promotes release of terminase from *cos* to initiate packaging. Vanadate traps ADP bound at the N/H ATPase site and prevents the conformational reorganization. Details of this model are presented in the text.

traps the gpA−ADP complex and interferes with the conformational reorganization to an activated enzyme complex described in Scheme 1. Thus, basal catalytic activities remain unaffected, but the ATP- and DNA-dependent transition to the activated complex is aborted. This model is fully consistent with the observation that the $K_{I,app}$'s for vanadate inhibition of DNA-stimulated ATPase, ATP-stimulated nuclease, and DNA helicase activities are quite similar. This suggests that a single molecular event is responsible for all of the allosteric interactions, and the model nicely accommodates the data. We note that the mechanism further predicts that neither DNA nor ATP binding steps will be affected by vanadate, which is precisely what is observed in this concentration range.

Nuclease Stimulation by Elevated Vanadate Concentrations. The above discussion focuses on events that occur at vanadate concentrations ≤600 μM. The concentration dependence observed for inhibition of nuclease and helicase activities of the holoenzyme suggests that a second mechanism is encountered at elevated vanadate concentrations. Moreover, any proposed kinetic model must accommodate the observation that millimolar concentrations of vanadate

stimulate the nuclease activity of the enzyme in the absence of ATP. Studies with phosphoryl transfer enzymes indicate that vanadate alone may bind to the catalytic site as a transition state analogue of phosphate (*43*, *44*). We speculate that VO_4^{3-} may directly interact with the empty phosphate binding pocket of the ATPase catalytic site and act as a transition state analogue of phosphate. Thus, in the absence of ATP vanadate binding may partially mimic nucleotide and stimulate nuclease activity. Importantly, millimolar concentrations of vanadate (but not phosphate) also inhibit AzATP labeling, which is consistent with competitive binding interactions with nucleotide triphosphate for the same site(s).

ATPase Activity of gpA in the Activated Holoenzyme. A mechanistic dissection of ATP hydrolysis by gpA is complex due to the fact that the subunit contains two ATPase catalytic sites (see Scheme 1). Studies with mutant terminases have demonstrated that the packaging ATPase gives rise to both basal and DNA-stimulated ATP hydrolysis (*24*, *28*). Thus, nucleotide interactions with the N/H ATPase site must be responsible for modulating the putative conformational reorganization and concomitant activation of the holoenzyme as described in Scheme 1. This includes an increase in ATP hydrolysis at the packaging ATPase site in gpA. We note, however, that the rate of ATP hydrolysis by the activated holoenzyme remains insufficient to power packaging of the genome (*8*, *29*), and this must represent only a partial activation of the site. Full expression of the packaging ATPase requires interaction of complex I with procapsids [Scheme 1 (*19*)], which are absent from the reaction mixture.

Helicase Activity in the Activated Complex. The model presented in Scheme 1 proposes that ADP bound at the N/H ATPase site is required to maintain the activated holoenzyme complex. What then "powers" strand separation in the so-called helicase reaction? We have previously proposed that the helicase activity is more appropriately described as a strand separation activity (*16*). In this model, ATP hydrolysis drives a conformational change to a complex that binds tightly and specifically to the single-stranded end formed by duplex nicking (*16*). This interaction would separate the nicked, annealed duplex and form a gpA complex tightly bound to the single-stranded end of the λ genome (Scheme 1). This is formally a single turnover of the active-rolling strand separation model proposed by Lohman and co-workers (*45*, *46*) and predicts that the strand separation activity of terminase does not require ATP *turnover*. ATP bound at the N/H ATPase site is hydrolyzed in a *single* catalytic cycle generating the gpA−ADP intermediate that has an increased affinity for the 12-base single-stranded "sticky" end formed in the duplex nicking reaction. Consistent with this proposed mechanism, no increase in the rate of ATP hydrolysis has been demonstrated as a result of strand separation by the terminase holoenzyme (*16*).

ATPase Activity of gpNu1 in the Activated Nuclease Complex. DNA stimulates ATP hydrolysis by gpNu1 in the holoenzyme complex (*23*, *26*). This DNA-stimulated activity is inhibited by vanadate with a $K_{I,app}$ essentially identical to that observed for inhibition of the ATPase, nuclease, and helicase activities of gpA. This is consistent with a linked molecular event that is responsible for global activation of the holoenzyme and that we attribute to the conformational reorganization described in Scheme 1. The function of the activated gpNu1 ATPase is unclear, but we suggest that this represents an assembly ATPase required for targeting the packaging machinery to *cos* and/or maintaining the stability of the nucleoprotein complex once formed.

The Packaging ATPase. In contrast to the essentially identical $K_{I,app}$'s for vanadate inhibition of activated ATPase, nuclease, and helicase activities of terminase, the $K_{I,app}$ for inhibition of DNA packaging is significantly greater. This is consistent with the observation that a discrete ATP binding site is associated with the packaging activity of the holoenzyme [Scheme 1 (*24*)]. The mechanism(s) leading to full activation of the packaging ATPase and translocation of terminase from the *cos* site during active DNA packaging remain(s) obscure. It is likely, however, that the packaging machine is composed of the terminase proteins in combination with portal proteins found in the procapsid. It is further likely that binding of the procapsid to complex I alters the structure and activity of the terminase subunits bound to viral DNA. We speculate that this interaction promotes ADP release from the nuclease/helicase ATPase site in gpA, which again alters the conformation of the proteins assembled at *cos*. We presume that this decreases the affinity of terminase for single-stranded DNA and concomitantly increases ATP hydrolysis at the packaging ATPase site thus driving translocation of the packaging machinery along the duplex.

Summary and Biological Significance. The ADP-mediated conformational reorganization proposed in Scheme 1 provides a unifying mechanistic explanation for our data and that previously published. With respect to the latter, it has been shown that ATP increases not only the rate but also the fidelity of the *cos*-cleavage reaction (*27*). We propose that the ADP-driven conformational reorganization appropriately "indexes" gpA at the nicking site (*cosN*), resulting in accurate duplex nicking. The model further accounts for the observation that ATP strongly affects the DNase footprint of terminase bound to *cos*-DNA (*36*). Conformational remodeling of the terminase subunits assembled at *cos* would necessarily lead to an alteration in the DNase protection pattern. The exact nature of the putative conformational reorganization is not clear, but it may involve a bone fide conformational change in the tertiary and/or quaternary structure of terminase holoenzyme, DNA wrapping by the proteins assembled at *cos*, and/or further assembly of higher order protein complexes on viral DNA.

Of what biological significance are these observed allosteric interactions? A series of nucleoprotein complexes are formed in the packaging of viral DNA (see Scheme 1). We have proposed that the initial assembly of terminase at *cos* is reversible and that an ADP-dependent conformational reorganization "locks" the proteins in place, forming a stable nuclease complex of high fidelity. Duplex nicking and a single-turnover helicase reaction yield complex I, a packaging intermediate in which the 12-base single-stranded end of the genome is protected by the terminase subunits tightly bound at *cos*. Premature release of DNA from this packaging intermediate would result in rapid degradation of the genome end and aborted virus replication. The stability of these prepackaging intermediates, which is likely modulated by ATP binding and/or hydrolysis by the holoenzyme, is thus critical to virus development. Procapsid binding to complex I triggers terminase release from *cos* and translocation of the packaging machinery as the duplex is inserted into the

capsid. Thus, terminase must switch from an extremely stable, site-specifically bound complex to a highly mobile packaging machine. This switch involves activation of a packaging ATPase activity and release of terminase from *cos*. We suggest that the ordered progression from one packaging intermediate to the next is regulated by ATP binding and/or hydrolysis at both subunits and that the observed allosteric behavior of terminase holoenzyme reflects these subtle interactions. These interactions are numerous and complex, and the present data do not allow a complete description at the molecular level. Nevertheless, the proposed model provides a framework for mechanistic dissection of the coordinated activities of λ terminase. While some details of this model will be specific to λ, it is likely that a general kinetic model will be universally applicable to all of the dsDNA viruses, just as general kinetic models have been developed in the characterization of DNA polymerase, RNA polymerase, and helicase enzymes from a variety of organisms.

ACKNOWLEDGMENT

The authors express their appreciation to Drs. Robert Kuchta, David Bain, and Michael Feiss for helpful discussions and critical review of the manuscript. We also thank the members of our laboratory for helpful discussions.

REFERENCES

1. Wood, W. R., and King, J. (1979) in *Comprehensive Virology* (Fraenkel-Conrat, H., and Wagner, R. R., Eds.) pp 581−611, Plenum Press, New York.
2. Casjens, S. R. (1985) in *Virus Structure and Assembly* (Casjens, S. R., Ed.) pp 1−28, Jones and Bartlett Publishers, Boston, MA.
3. Fields, B. N., Knipe, D. M., and Howley, P. M. (1996) *Fields Virology*, 3rd ed., Lippincott-Raven, Philadelphia, PA.
4. Earnshaw, W. C., and Casjens, S. R. (1980) *Cell 21*, 319−331.
5. Black, L. W. (1989) *Annu. Rev. Microbiol. 43*, 267−292.
6. Roizman, B., and Sears, A. E. (1996) in *Fields Viriology* (Fields, B. N., Knipe, D. M., and Howley, P. M., Eds.) pp 2231−2297, Lippencott-Raven, New York.
7. Droge, A., and Tavares, P. (2000) *J. Mol. Biol. 296*, 103−105.
8. Catalano, C. E. (2000) *Cell. Mol. Life Sci. 57*, 128−148.
9. Becker, A., and Murialdo, H. (1990) *J. Bacteriol. 172*, 2819−2824.
10. Feiss, M. (1986) *Trends Genet. 2*, 100−104.
11. Gold, M., and Becker, A. (1983) *J. Biol. Chem. 258*, 14619−14625.
12. Tomka, M. A., and Catalano, C. E. (1993) *J. Biol. Chem. 268*, 3056−3065.
13. Becker, A., and Gold, M. (1978) *Proc. Natl. Acad. Sci. U.S.A. 75*, 4199−4203.
14. Rubinchik, S., Parris, W., and Gold, M. (1994) *J. Biol. Chem. 269*, 13575−13585.
15. Parris, W., Rubinchik, S., Yang, Y.-C., and Gold, M. (1994) *J. Biol. Chem. 269*, 13564−13574.
16. Yang, Q., and Catalano, C. E. (1997) *Biochemistry 36*, 10638−10645.
17. Rubinchik, S., Parris, W., and Gold, M. (1995) *J. Biol. Chem. 270*, 20059−20066.
18. Hwang, Y., and Feiss, M. (1995) *Virology 211*, 367−376.
19. Yang, Q., and Catalano, C. E. (2003) *Virology 305*, 276−287.
20. Rubinchik, S., Parris, W., and Gold, M. (1994) *J. Biol. Chem. 269*, 13586−13593.
21. Hwang, Y., Catalano, C. E., and Feiss, M. (1996) *Biochemistry 35*, 2796−2803.
22. Yang, Q., Hanagan, A., and Catalano, C. E. (1997) *Biochemistry 36*, 2744−2752.
23. Tomka, M. A., and Catalano, C. E. (1993) *Biochemistry 32*, 11992−11997.
24. Hang, J. Q., Tack, B. F., and Feiss, M. (2000) *J. Mol. Biol. 302*, 777−795.
25. Babbar, B. K., and Gold, M. (1998) *Virology 247*, 251−264.
26. Woods, L., and Catalano, C. E. (1999) *Biochemistry 38*, 14624−14630.
27. Higgins, R. R., Lucko, H. J., and Becker, A. (1988) *Cell 54*, 765−775.
28. Hwang, Y., and Feiss, M. (1996) *J. Mol. Biol. 261*, 524−535.
29. Catalano, C. E., Cue, D., and Feiss, M. (1995) *Mol. Microbiol. 16*, 1075−1086.
30. Goodno, C. C. (1982) *Methods Enzymol. 85*, 116−123.
31. Hang, J. Q., Woods, L., Feiss, M., and Catalano, C. E. (1999) *J. Biol. Chem. 274*, 15305−15314.
32. Nash, H. A., Robertson, C. A., Flamm, E., Weisberg, R. A., and Miller, H. I. (1987) *J. Bacteriol. 169*, 4124−4127.
33. Woods, L., Terpening, C., and Catalano, C. E. (1997) *Biochemistry 36*, 5777−5785.
34. Sankaran, B., Bhagat, S., and Senior, A. E. (1997) *Arch. Biochem. Biophys. 341*, 160−169.
35. Czarnecki, J., Geahlen, R., and Haley, B. (1979) *Methods Enzymol. 61*, 642−653.
36. Higgins, R. R., and Becker, A. (1995) *J. Mol. Biol. 252*, 31−46.
37. Cue, D., and Feiss, M. (1993) *J. Mol. Biol. 234*, 594−609.
38. Mendelson, I., Gottesman, M., and Oppenheim, A. B. (1991) *J. Bacteriol. 173*, 1670−1676.
39. Granston, A. E., Alessi, D. M., Eades, L. J., and Friedman, D. I. (1988) *Mol. Gen. Genet. 212*, 149−156.
40. Feiss, M., Fogarty, S., and Christiansen, S. (1988) *Mol. Gen. Genet. 212*, 142−148.
41. Fujisawa, H., and Morita, M. (1997) *Genes Cells 2*, 537−545.
42. Urbatsch, I. L., Sankaran, B., Weber, J., and Senior, A. E. (1995) *J. Biol. Chem. 270*, 19383−19390.
43. Deng, H., Callendar, R., Huang, Z., and Zhang, Z.-Y. (2002) *Biochemistry 41*, 5865−5872.
44. Lindquist, R. N., Lynn, J. L., and Lienhard, G. E. (1973) *J. Am. Chem. Soc. 95*, 8762−8768.
45. Lohman, T. M. (1993) *J. Biol. Chem. 268*, 2269−2272.
46. Wong, I., and Lohman, T. M. (1992) *Science 256*, 350−355.

BI035532H